mathematics

Article

Numerical Analysis and Parametric Optimization of T-Shaped Symmetrical Metasurface with Broad Bandwidth for Solar Absorber Application Based on Graphene Material

Meshari Alsharari *, Ammar Armghan * and Khaled Aliqab

Department of Electrical Engineering, College of Engineering, Jouf University, Sakaka 72388, Saudi Arabia
* Correspondence: mmaalsharari@ju.edu.sa (M.A.); aarmghan@ju.edu.sa (A.A.)

Abstract: Solar energy is an essential renewable energy source among all the other renewable energy sources. It is possible to improve the efficiency of the solar energy absorber by increasing the solar energy absorber's capacity for absorption, which can help in building better solar-based renewable energy devices. The need of covering the whole solar spectrum led us to design this T-shaped metasurface solar absorber which is based on graphene material. The T-shaped absorber gives 90, 88 and 57% absorption in the visible, infrared and UV regions, respectively. This symmetrical structure is also periodic with respect to x-axis and y-axis. This solar absorber demonstrates better efficiency compared to many other existing solar absorbers. The solar absorber is also compared with two other square-1 and square-2 designs to show the improvement in solar energy absorption. The parametric optimization method is applied to optimize the design. The parameters, such as the length and width of the substrate and the thicknesses of the T-shaped metasurface and substrate, are varied to find out the optimized design for maximum solar energy absorption. The optimized parameters obtained from the optimization are 1000, 2500, 3000 and 3000 nm, for resonator thickness, substrate thickness, substrate length and substrate width, respectively. The design results for graphene material and its potential variation are also observed. The design also shows good absorption for a wide-angle of incidence of about 0 to 50°. The increased efficiency of this design can be applied in future solar absorber devices.

Keywords: numerical optimization; parametric optimization; computational; finite element analysis; solar energy; absorber; photovoltaic applications

MSC: 65K10; 78-10; 00A06

check for updates

Citation: Alsharari, M.; Armghan, A.; Aliqab, K. Numerical Analysis and Parametric Optimization of T-Shaped Symmetrical Metasurface with Broad Bandwidth for Solar Absorber Application Based on Graphene Material. *Mathematics* **2023**, *11*, 971. https://doi.org/10.3390/math11040971

Academic Editors: André Nicolet and Guillaume Demésy

Received: 23 January 2023
Revised: 4 February 2023
Accepted: 11 February 2023
Published: 14 February 2023

1. Introduction

Renewable energy sources are gaining interest among researchers because of limited fossil fuel resources [1]. One more disadvantage of using fossil fuels is it increases pollution while the renewable resources are clean and sustainable [2]. Solar power is widely recognized as one of the most significant examples of currently available forms of renewable energy and the absorber converts solar energy into heat energy [3]. The solar energy efficiency in the solar absorber can be improved by applying the mathematical optimization methods such as parametric optimization [4]. This heat energy can be used in many day-to-day life applications as well as industrial applications. The solar absorbers' efficiency is very important and most of the absorbers are absorbing the energy of the visible spectrum [5]. There is a need for a solar absorber to absorb visible, ultraviolet and infrared spectrum energy. The need for this broad spectrum and high efficiency can be met by using metamaterials and graphene material, which are novel concepts that can be incorporated into traditional solar absorber designs to meet the high efficiency and broadband requirement of today's solar absorbers.

Metamaterials are important man-made materials with unexpected features such as negative permittivity and permeability [6]. Metamaterials can be used with their unusual properties to improve the solar absorber designs' efficiency [7–9]. The split ring resonators (SRR) are one of the components of metamaterials that can be used for designing, the second component is thin wires and the third counterpart of SRR is complementary split-ring resonators, etc., which can be supplemented to make the solar absorber more effective. The SRR-based approach is shown in [10] and a thin wires-based solar cell design with CZTS thin film is presented in [11]. A split hexagonal patch array has been used as a metamaterial absorber to absorb not only visible but also ultraviolet regions [12]. A gold resonator array placed over a substrate is used to improve the absorption and create a broadband near-infrared absorber [13]. Gold is used to create a solar absorber that is a near-infrared and near-visible metamaterial absorber [14]. Absorption of light can be increased using plasmonic grating, which can be used to get broadband absorptions [15]. The solar thermal absorber is designed using a MIM sandwiched structure with nanodisks to overcome the limitations of existing plasmonic metamaterial absorbers [16]. The symmetrical structures show a better response, which can be used to improve the absorption. Symmetrical metasurfaces improve the absorption of an absorber. The symmetric structures are also able to show a multiband response in the absorber structure [17]. The symmetrical array of the metamaterial structures is used for flat lenses. The twisted symmetries are used for this with a complementary split ring resonator [18]. The concept of symmetrical structures is also used to improve the sensing of sensors for the THz frequency band region [19]. Metamaterials can be designed with different metals and materials. The metamaterial design with Nickel [20], GST [21], Vendium dioxide [22], Tantalum carbide [23], tungsten [24], Al-doped ZnO [25] and TiN [26] are used for solar absorbers and solar thermal applications.

Graphene is an exceptional electrical and optical material because it is only one atom thick in nature, which can be used in a variety of applications to improve the efficiency of solar absorbers [27–29]. A graphene spacer can be added between the resonator and the substrate to boost the solar absorber's absorption [30]. Graphene, with its excellent optical properties, can be useful in energy-storing devices [31]. A broadband solar absorber covering most of the solar spectral visible region is designed using a graphene metasurface-based solar absorber [32]. To achieve a wider absorption bandwidth in the near-infrared, reduced graphene oxide is used with composites of TiO_2 to create a broadband solar absorber [33]. The O-shape gold material design which is placed on a substrate base outperforms the L-shape gold material design in terms of performance in designing solar absorbers with exceptional performance. To demonstrate the solar absorber's effectiveness, AM 1.5 solar spectrum irradiance is used to compare absorption performance. The designs are also verified for different parameters with optimization. The graphene spacer layer is layered on the top of the substrate and beneath the metasurface material to achieve broadband absorption [34]. Zirconium nitride metamaterial absorber is suggested for better absorption characteristics. The suggested absorber has ZrN circular nanodisks created to generate the metasurface effect laid over a SiO2 substrate [35]. Multilayer metasurface designs can also improve the absorption and a broad spectral absorption range can be achieved. One such absorber based on a swastika-shaped metasurface layer is analyzed by researchers to improve the absorption [36].

The graphene material can be mixed in the different road-creating materials for better improvement and performance of roads. The graphene material can also be used with its anti-aging enhancing properties in modified asphalt [37]. The graphene-based asphalt can be used in creating roads, which produces better quality and performance [38]. The different defects of cement products can be analyzed and improved using the addition of graphene [39]. The graphene material can also be used in designing smart composites. The graphene nanoplatelets can be used for that purpose [40]. Graphene can be used for electrochemical applications [41]. Microwave-assisted heating with graphene material can be suitable for carbon precursors [42].

Mathematical optimization methods can be applied to solve different problems in electromagnetic and photonics problems [43]. One such method is the optimization method where parametric optimization can be applied to optimize the design to get better results [44]. Machine learning and deep learning optimization algorithms are also used to optimize the design results. The elephant herding optimization algorithm is used to optimize the design and produce better results [45]. The parameters are tuned to optimize the available results. The tuning of parameters is done with different algorithms [46]. The photovoltaic designs and their models are optimized by applying parametric optimization to these models. The optimization improves the efficiency of the models [47]. Parametric optimization is the mathematical optimization method used to optimize the results where the parameters of physical or geometrical nature are required to be optimized. These two optimization methods known as linear parametric optimization method and nonlinear parametric optimization method are used based on the behavior of the response. These optimization methods are used to optimize the response and improve the results of the absorber or other structures [48].

The solar absorber design requires high efficiency and broad bandwidth that covers all solar regions. We propose a solar absorber that is broadly effective against solar radiation covering 0.2 to 1.5 nm. The efficiency of this solar absorber is also good with the highest average absorption of 95% with the visible spectrum. The metasurface design is also optimized with several solar absorber physical variables to get the highest efficiency for the design. The effects of the electric field are equally interesting and obtained to observe the high electric energy in the proposed structure. The proposed structure analysis and its results, which can be found in Sections 2 and 3. The fourth portion contains final observations.

The main objectives of this research are (1) Design of an efficient solar absorber that can absorb not only visible but UV and infrared regions. (2) The structural optimization of the solar absorber design to improve the overall efficiency of the solar absorber. (3) Use of the metasurface structure to improve the efficiency and reduce the structure size. (4) Design of a metasurface structure which is easy to fabricate with less complexity and cost.

2. Design and Modeling

We have presented our proposed solar absorber design in Figure 1. We have verified three metasurface designs to observe the highest absorption for the absorber design. The results for the T-shape metasurface design are compared with square-1 metamaterial design and square-2 metamaterial designs. The metasurface shape is varied and the results are observed for these three metasurface designs. The metasurface designs are observed to check whether our T-shape design is performing better than the other designs or not. Section 3 contains the outcomes of all the designs. The two designs from the top are shown in Figure 1a,b and the design is shown from the front in Figure 1c. The graphene layer is inserted between the metasurface and substrate as presented in Figure 1c. The size of the different physical parameters of the designs is denoted by X1, X2, X3 and X4 and is given by 3000, 2500, 1000 and 2800 nm. The T-shape size and square-1 size are kept the same and it is 2500 nm. In the next part of this section, the graphene layer is a single atom thick and has a thickness of 0.34 nm. We have presented the numerical analysis of the absorption and graphene materials. The design presented in Figure 1 is the optimized design which is obtained by checking various designs and their results. The three different designs are shown in the figure. One has the square resonator covering most of the part of the substrate while the second square resonator has shorter length and width compared to the substrate. The etching of two rectangular slits from the square resonator creates the T-shape metamaterial design, which is presented in Figure 1a, and the results of all three designs are shown and compared in the upcoming section. The analysis of the absorption and graphene parameters is provided here for better understanding. The absorption of the structure is dependent on the amount of reflection and transmittance. The angle of incidence is also playing the vital role in the absorption of the solar energy. The detailed analysis of the abruption is provided here.

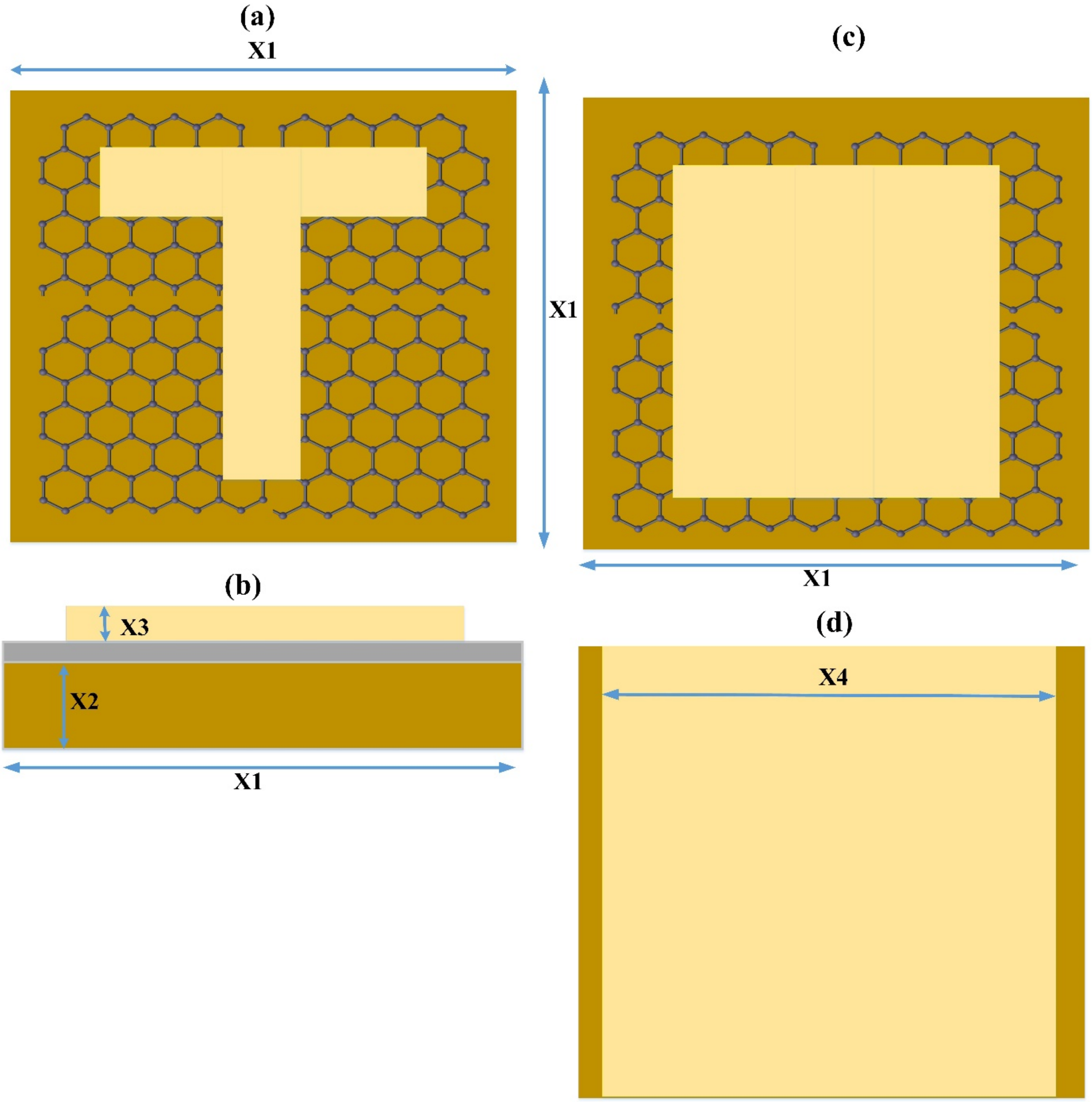

Figure 1. Solar absorber design with three different metasurfaces. (**a**,**b**) T-shape metasurface absorber. (**c**) Square-1 metasurface absorber design. (**d**) Square-2 metasurface absorber design. The design parameter values are X1 = 3000 nm, X2 = 2500 nm, X3 = 1000 nm, X4 = 2800 nm. The T-shape length and width are 2500 nm and square-1 shape size is also 2500 nm.

2.1. Analysis of Absorption

Absorption depends on reflectance and transmittance. As these two values reduce, the absorption increases. The reflectance and its dependence on the incidence angle are presented in [49].

$$r(\omega, \theta_i) = \frac{\omega \cos\theta_i \prod_{00}(\omega, \theta_i)}{2i\hbar ck^2 + \omega \cos\theta_i \prod_{00}(\omega, \theta_i)} \quad (1)$$

$$\sigma_{||}(\omega,k) = -i\,\frac{\omega}{4\pi\hbar k^2}\prod\nolimits_{00}(\omega,k) \tag{2}$$

$$r(\omega,\theta_i) = \frac{2\pi\cos\theta_i\sigma_{||}(\omega,k)}{c+2\pi\cos\theta_i\sigma_{||}(\omega,k)} \tag{3}$$

$$\mathcal{R}(\omega,\theta_i) = |r(\omega,\theta_i)|^2 \tag{4}$$

$$\mathcal{R}(\omega,\theta_i) = \frac{4\pi^2\cos^2\theta_i\left[\mathrm{Re}^2\sigma_{||}(\omega,k)+\mathrm{Im}^2\sigma_{||}(\omega,k)\right]}{\left[c+2\pi\cos\theta_i\mathrm{Re}\sigma_{||}(\omega,k)\right]^2+4\pi^2\cos^2\theta_i\mathrm{Im}^2\sigma_{||}(\omega,k)} \tag{5}$$

$$\mathcal{R}(\omega) = \mathcal{R}(\omega,0) = \frac{4\pi^2\left[\mathrm{Re}^2\sigma(\omega)+\mathrm{Im}^2\sigma(\omega)\right]}{[c+2\pi\mathrm{Re}\sigma(\omega)]^2+4\pi^2\mathrm{Im}^2\sigma(\omega)} \tag{6}$$

$$A(\omega) = 1-\mathcal{R}(\omega)-T(\omega) \tag{7}$$

2.2. Analysis of Graphene

The graphene conductivity depends mainly on its chemical potential and its dependence is provided in [50]. The graphene material majorly depends on the graphene layer conductivity for tuning its spectrum and also achieving the higher absorption results. The tuning of the result is achieved by giving a change in graphene potential that is applied to the monolayer graphene sheet. The graphene layer and its applied potential also helps in achieving the higher absorption, which can be utilized for the solar absorber to improve its efficiency.

$$\varepsilon(\omega) = 1+\frac{\sigma_s}{\varepsilon_0\omega\Delta} \tag{8}$$

$$\sigma_{intra} = \frac{-je^2k_BT}{\pi\hbar^2(\omega-j2\Gamma)}\left(\frac{\mu_c}{k_BT}+2ln\left(e^{-\frac{\mu_c}{k_BT}}+1\right)\right) \tag{9}$$

$$\sigma_{inter} = \frac{-je^2}{4\pi\hbar}ln\left(\frac{2|\mu_c|-(\omega-j2\Gamma)\hbar}{2|\mu_c|+(\omega-j2\Gamma)\hbar}\right) \tag{10}$$

$$\sigma_s = \sigma_{inter}+\sigma_{intra} \tag{11}$$

3. Design and Results

Using COMSOL Multiphysics, the design depicted in Figure 1 is analyzed and simulated, and analyzed results are presented in upcoming figures. Absorption, electric field, different geometrical parameter variation, incident angle variation and graphene potential variation are all examples of the outcomes. The three metasurface designs are investigated and Figure 2 shows the outcomes of the experiment by means of absorbing, and its numerical values for different solar spectral regions are shown in Table 1. The absorption of the solar absorber mainly depends on the three layers of Titanium-graphene-SiO_2. These three layers absorb solar energy. The absorption is achieved initially with a resonator of titanium which further increases because of graphene's high optical and electrical properties. The base of the SiO_2 substrate absorbs the amount of energy that is passed through the titanium and graphene layers. We have not used any ground metal plane, yet we are achieving more than 90% average absorption. The resonator is made up of Titanium material and the substrate is made up of SiO_2 material. The data shown in Figure 2 demonstrate that the absorption of the T-shape metasurface has better results compared to square-1 and square-2 designs. The T-shape metasurface design results are presented in Figure 2a. It is obvious from the findings that the absorption is about on average 90% to 1.6 micrometer range. In the ultraviolet region, 57% absorption is accomplished, 90% in the visible range and 88% is in the infrared range of 0.7 m to 1.6 m. The data are also listed in Table 1 for comparison purposes. The square-1 design findings suggest that the design results in terms of absorption degradation as the T-shape is converted to the whole square shape. The reason for this result degradation is change in inductance because of the increase in the metal part of the absorber design. In the ultraviolet region, 60% absorption is accomplished, 71% in the visible range, and 72% in the infrared range of 0.7 m to 1.6 m. The design results further degrade as the size of the square shape is increased and square-2 metasurface design is investigated. In the ultraviolet region, 55% absorption is accomplished, 62%in the visible range, and 40% in the infrared range of 0.7 m to 1.6 m. The design results show that the absorption is reduced to less than 70% above 1.6 μm so we have taken the absorption between 0.2 and 1.6 micrometers for all the next result discussions for the parameter variation and its effect on the absorption.

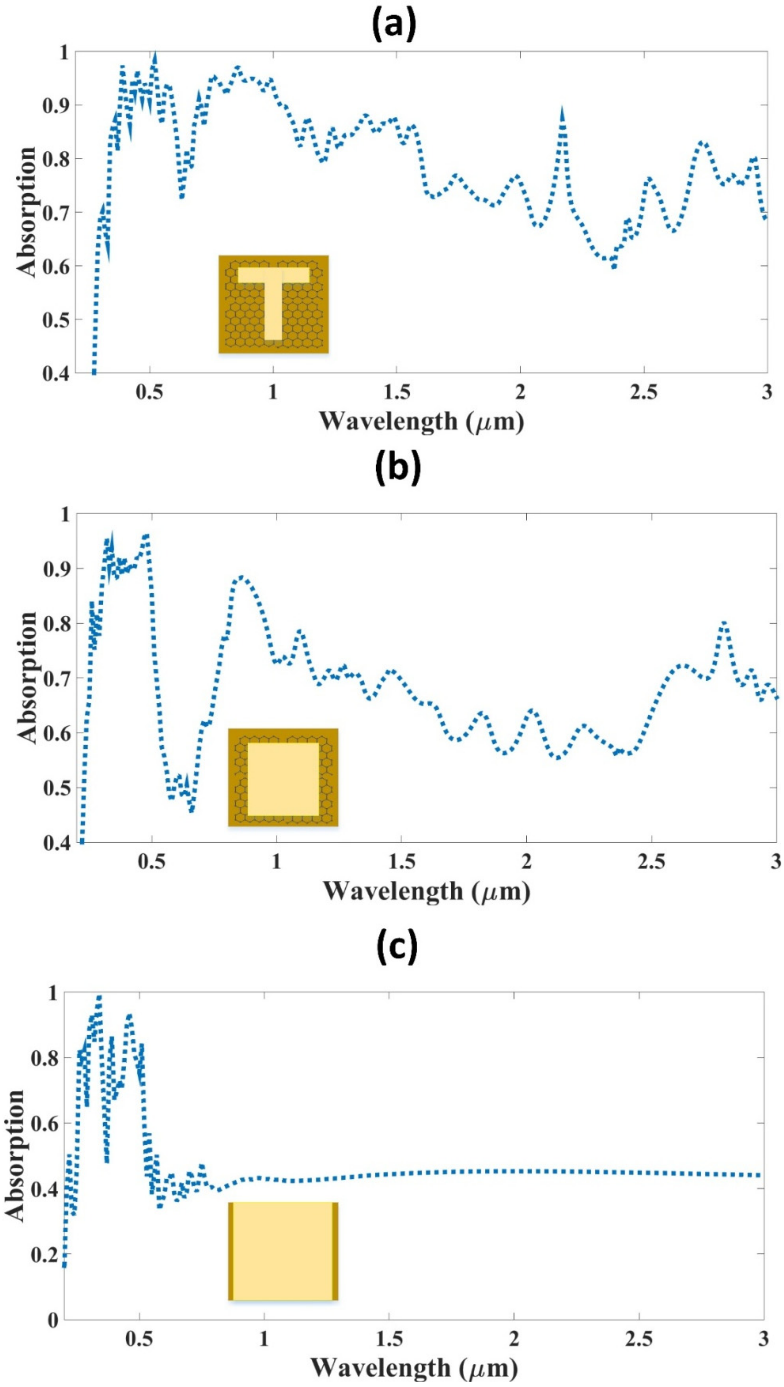

Figure 2. Absorption results for different metasurface solar absorbers. (**a**) T-shape metasurface design. (**b**) Square-1 metasurface shape design. (**c**) Square-2 metasurface shape design.

Table 1. Comparison of the proposed metasurface design results.

	0.2 to 0.4 (Micrometer) (Avg. Absorption in %)	0.4 to 0.7 (Micrometer) (Avg. Absorption in %)	0.7 to 1.6 (Micrometer) (Avg. Absorption in %)
T-shape metasurface design	57	90	88
Square-1 metasurface design	60	71	72
Square-2 metasurface design	55	62	40

Parametric Optimization

It is possible to use an optimization technique known as parametric optimization to observe the effect of improvement in absorption which can increase the effectiveness of the design. Here, we have applied the nonlinear optimization of the solar absorber which can usually match well with the nonlinear behavior of the solar absorption response. The optimization of the solar absorber is mainly done by optimizing the geometrical parameters of the solar absorber such as resonator thickness, substrate thickness, substrate length and width [51].

The functions do not behave linearly, which produces this optimization. It has function $f(x)$, constraint $c_i(x) = 1, 2, \ldots\ldots..n$ or $d_j(x) = 1, 2, \ldots\ldots..n$ are components of x that are non linear.

The different geometrical parameters such as substrate height, resonator and length and width of the substrate are analyzed for the T-shape metasurface absorber design. The parametric optimization produces the best possible results for absorption. The resonator height and the substrate height and its variation results are presented in Figure 3. The responses are analyzed for the wavelength range of 0.2 to 1.6 micrometers. The absorption results show that the initial wavelength is from 0.2 to 0.3 micrometer and the absorption is around 90% for the other part. As the resonator thickness rises the absorption rises. The highest absorption is visible in the resonator thickness of 1000 nm with red color plot. The resonator helps in the concentration of the solar radiation in substrate. The rise in the substrate thickness rises the absorption as it will help in absorbing the radiation more. The rise in substrate thickness rises the absorption and it is visible in Figure 3b.

For the geometrical parameters such as length and width of the substrate and its variation, the data are reported in the form of absorption in Figure 4. The results are analyzed for the wavelength range of 0.2 to 1.6 micrometers. The absorption results show that the initial wavelength is from 0.2 to 0.3 micrometer and the absorption is decreasing two parameters. As the substrate length and width decrease, the absorption rises. The highest absorption is visible in the substrate length of 3000 nm and substrate width of 3000 nm. The rise in substrate length and width rises the absorption and it is visible in Figure 4. The variation in length and width are presented in Figures 4a and 4b, respectively. The red color indicates the rise in absorption and the blue color indicates less absorption.

Graphene is very essential in boosting the solar absorber's absorption. The change in graphene potential can affect the overall absorption that's why the variation in graphene chemical potential is also carried out to show that there is no change in absorption levels for the investigated wavelength range. Figure 5 depicts the outcomes for this variation. The potential of graphene is changed between 0.1 and 0.9 eV. The wavelength range is 0.2 to 1.6 micrometer. The absorption outcomes are evident that the vertical lines of red color for good absorption and blue color vertical lines for less absorption. The vertical lines illustrate that increasing the graphene chemical potential does not affect the results. The potential variation does not affect the solar absorber's efficiency.

The angle of incidence is very important in absorbing solar radiation as the sun changes its position throughout the day, we have investigated the absorption variation for varying incidence angles. In Figure 6, the incidence angle is changed from 0 to 80° to see how it affects the overall absorption. The results from the figure clearly show that the absorption is considerable for incidence angles of 0 to 50° and for the other angles, the absorption is decreasing. The solar absorber shows a wide angle of incidence of 0 to 50° for the T-shape metasurface design.

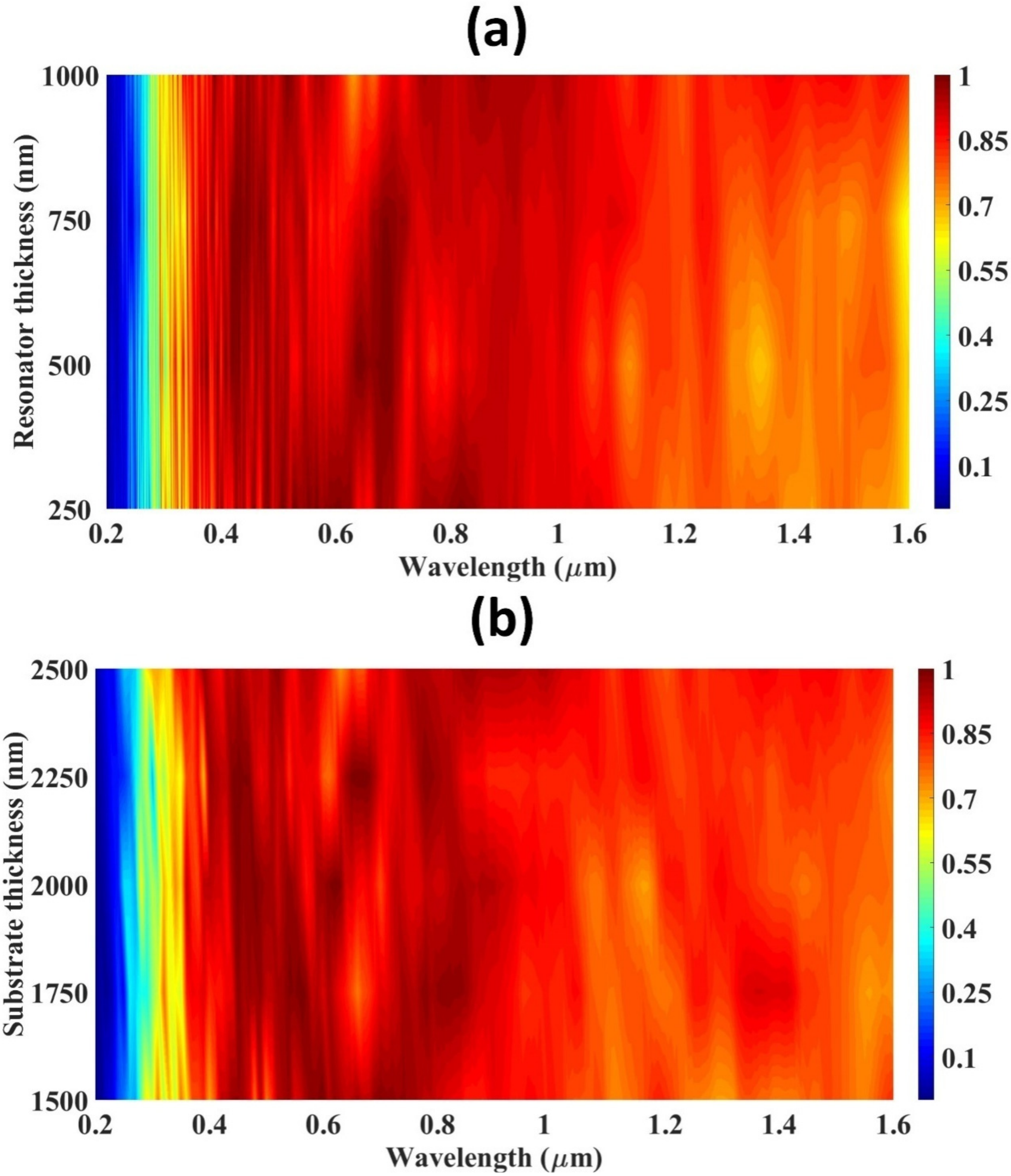

Figure 3. Parameter variation for the 0.2 to 1.6 micrometer spectrum. (**a**) Resonator thickness (nm). (**b**) Substrate thickness (nm). The absorbance increases as the resonator and substrate thicknesses grow. The best value of resonator and substrate thickness is 1000 and 2500 nm, respectively.

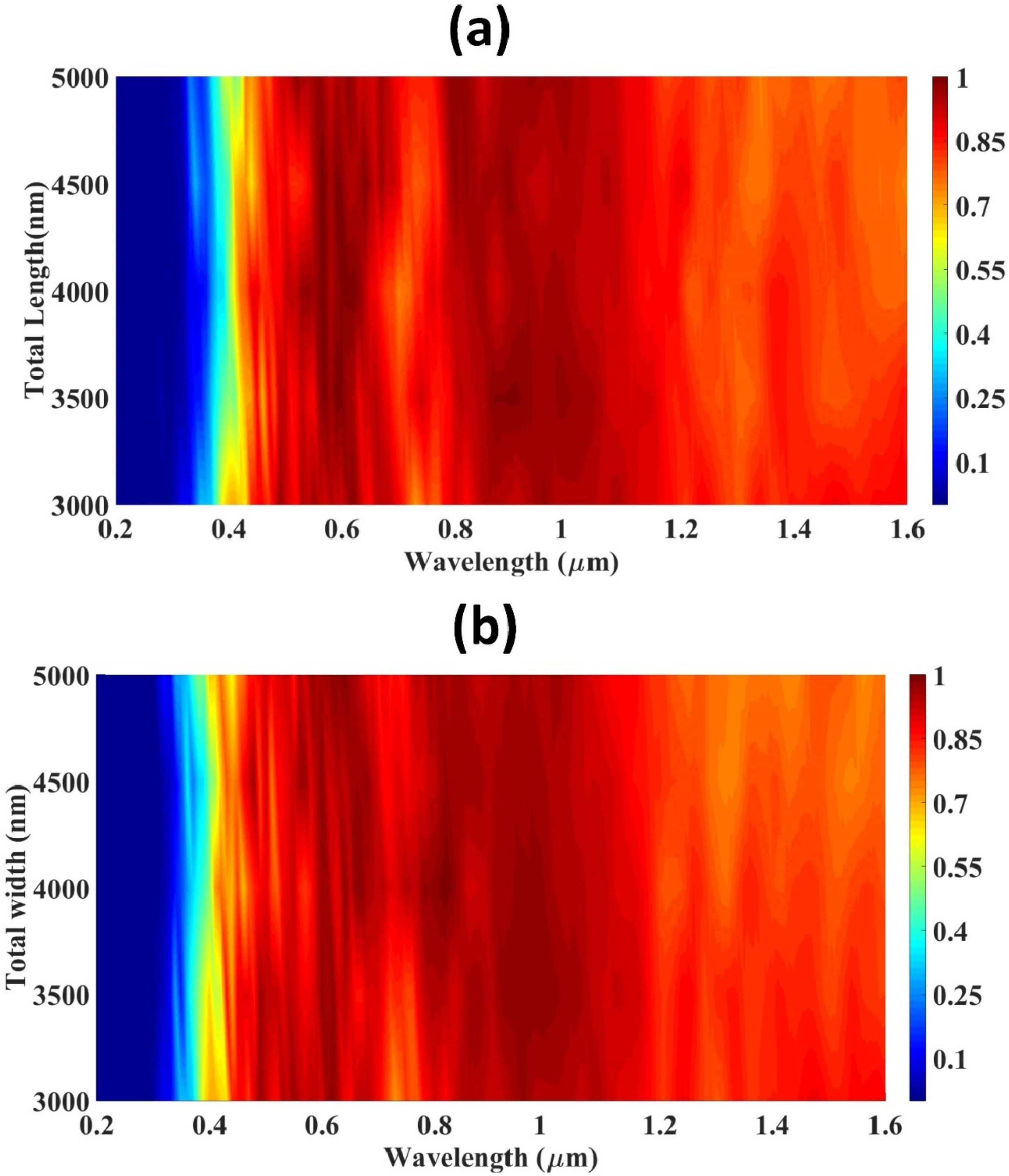

Figure 4. Parameter variation for the range of 0.2 to 1.6 micrometers. (**a**) Total length (nm). (**b**) Total width (nm). The increase in length and width of the substrate decreases the absorption. The optimized value of the total length and width of the substrate are 3000 nm each.

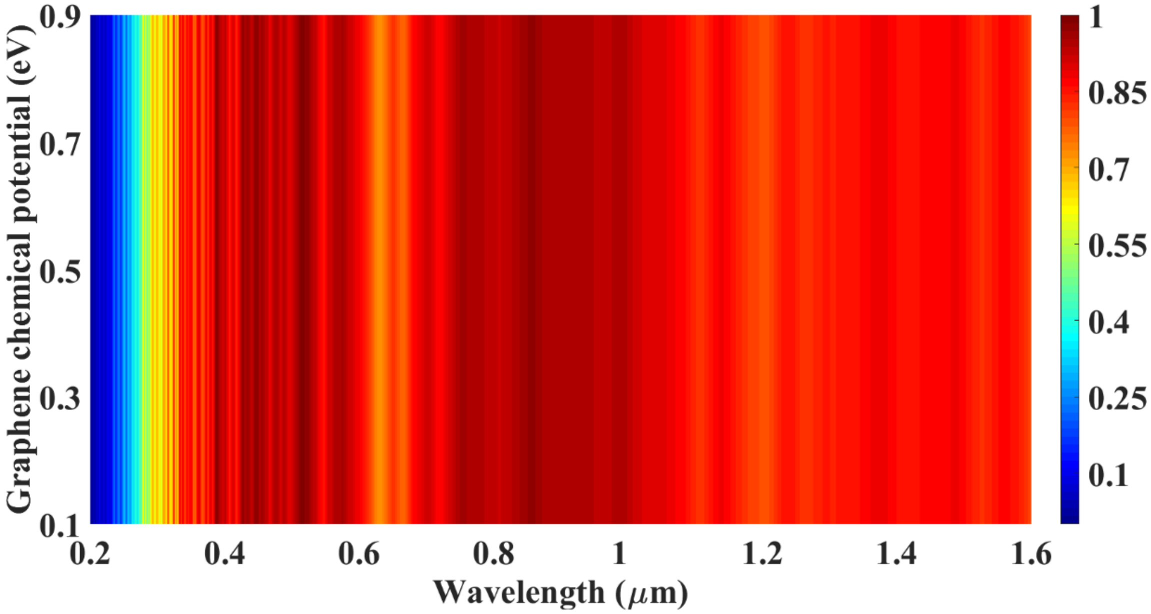

Figure 5. The graphene's potential variation results. The wavelength spectrum of 0.2 micrometer to 1.6 micrometer. The chemical potential of graphene is changed between 0.1 and 0.9 eV. For varied graphene chemical potentials, the absorption remains unchanged.

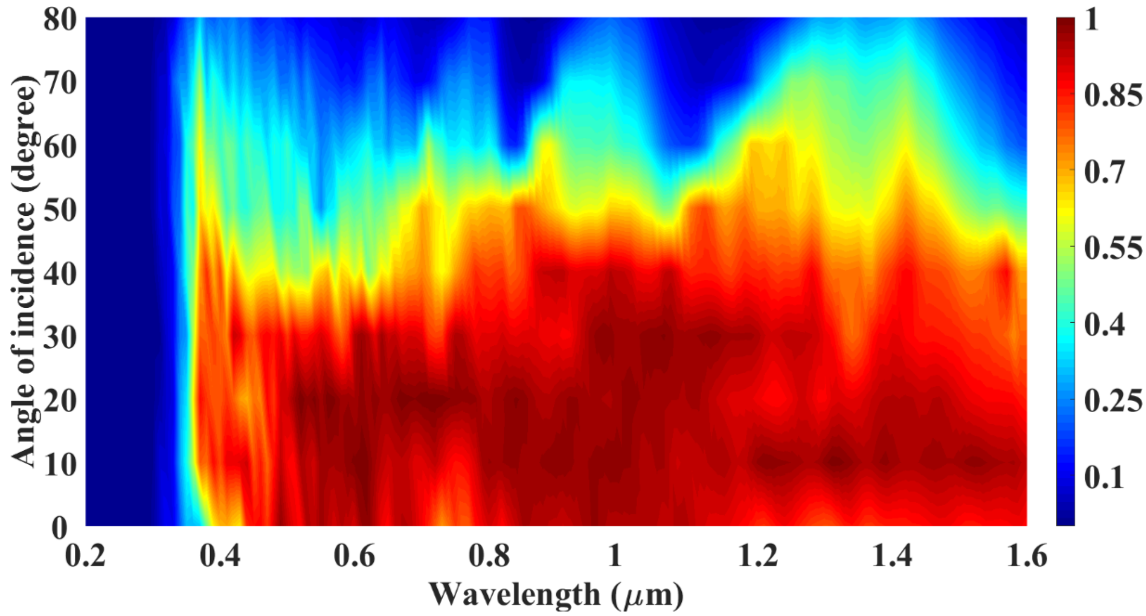

Figure 6. The angle of incidence variation absorption results. The wavelength spectrum of 0.2 to 1.6 micrometers. The angle of incidence is varied from 0 to 80°. A wide angle of incidence of 0 to 50° is available for this T-shape metasurface solar absorber design.

The electric field is another important parameter that needs to be investigated to check the absorption of different wavelengths. Here, we investigated electric field results for three different wavelengths: 0.25, 0.50 and 0.75 micrometer as shown in Figure 7. The absorption results are matching with the electric field results for all three wavelengths. The three wavelengths were chosen to observe the electric field at various places across the spectrum. The comparison of the T-shape metasurface absorber design is also compared with the design results of [24–33] as presented in Table 2 and the results show promising absorption compared to other design results. The comparison of the designs shows that there are designs with around 90% absorption for a visible region such as ours but those designs do not give any absorption in ultraviolet or infrared regions while our designs give 57% for the ultraviolet region and 88% for the infrared region. Thus, our design has overall good absorption compared to the other designs presented or published previously. The design complexity of our design is also less and the materials used are also available and can be fabricated easily for the solar thermal energy conversion devices.

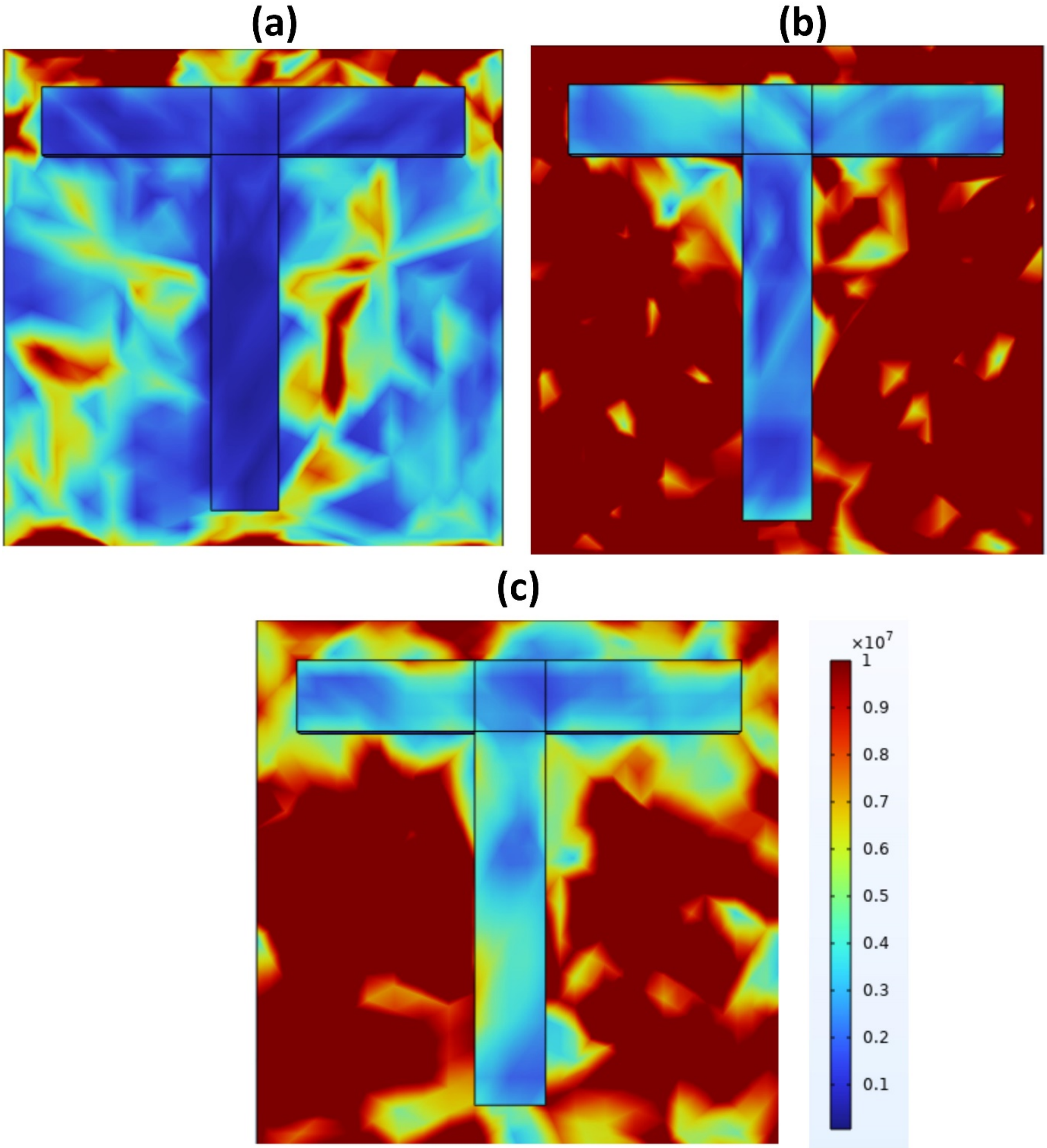

Figure 7. E-field results for wavelengths: (**a**) 0.25 micrometer, (**b**) 0.50 micrometer, (**c**) 0.75 micrometer.

Table 2. The analysis of the three designs with other designs.

Designs	0.2 to 0.4 (Micrometer) (Avg. Absorption in %)	0.4 to 0.7 (Micrometer) (Avg. Absorption in %)	0.7 to 1.6 (Micrometer) (Avg. Absorption in %)
T-shape metasurface design	57	90	88
Square-1 metasurface design	60	71	72
Square-2 metasurface design	55	62	40
Refrectory Metal design [52]	-	90	-
Array of C-shaped metasurface design [29]	-	86.5	-
90 nm thick graphene absorber design [53]	-	93	-
Broadband metasurface design [54]	-	90	-
Monolayer graphene design [55]	-	80	-
Multi grooved metasurface design [56]	-	71.1	-
Meta absorber for solar cell design [57]	-	70	-
Solar cell design [58]	-	84	77
Broadband absorber design [59]	-	93.7	-

4. Conclusions

We studied three different metasurface designs to find a highly efficient T-shape metasurface solar absorber design. The design response is analyzed for absorption, electric field and parametric optimization. The results for these three metasurface designs (T-shape, square-1 and square-2) are also compared to observe the improved proposed design. The mathematical nonlinear parametric optimization method is applied to optimize the parameters and obtain a higher efficiency for the solar absorber design. The comparison clearly shows that a T-shape design has the maximum absorption with an average absorption of 57, 90 and 88% in the ultraviolet region, visible region and infrared region of 0.7 to 1.6 µm. The parameter optimization led to the best values of resonator thickness of 1000 nm, resonator thickness of 2500 nm and substrate length and width of 3000 nm each. The T-shape metamaterial design shows a wide angle of incidence in the range of 0 to 50°. The electric field analysis presented shows the absorption behavior presented in the T-shape design. The design can further be improved in the future to absorb more of the UV spectrum energy and also increase the efficiency of visible and infrared spectrum absorption to make perfect absorption. This can be achieved by improving the design using a new metamaterial approach and graphene metasurface concepts.

Author Contributions: Conceptualization, M.A. and A.A.; methodology, K.A.; software, M.A. and A.A.; validation, M.A.; formal analysis, A.A. and K.A.; investigation, M.A. and A.A.; resources, M.A. and A.A.; writing—original draft preparation, all authors; writing—review and editing, all authors. All authors have read and agreed to the published version of the manuscript.

Funding: The authors extend their appreciation to the Deputyship for Research & Innovation, Ministry of Education in Saudi Arabia for funding this research work through the project number 223202.

Data Availability Statement: The data will be made available at a reasonable request to corresponding author.

Conflicts of Interest: The authors declare no conflict of interest.

Abbreviations

Abbreviations	**Full Form**
UV	Ultraviolet
SRR	Split ring resonator
CZTS	Copper zinc tin sulfide
MIM	Metal Insulator Metal
GST	Germanium-Antimony-Tellurium
ZnO	Zinc Oxide
Avg	Average

References

1. Li, L.; Lin, J.; Wu, N.; Xie, S.; Meng, C.; Zheng, Y.; Wang, X.; Zhao, Y. Review and Outlook on the International Renewable Energy Development. *Energy Built Environ.* **2022**, *3*, 139–157. [CrossRef]
2. Elavarasan, R.M.; Shafiullah, G.M.; Padmanaban, S.; Kumar, N.M.; Annam, A.; Vetrichelvan, A.M.; Mihet-Popa, L.; Holm-Nielsen, J.B. A Comprehensive Review on Renewable Energy Development, Challenges, and Policies of Leading Indian States With an International Perspective. *IEEE Access* **2020**, *8*, 74432–74457. [CrossRef]
3. Novas, N.; Garcia, R.; Camacho, J.; Alcayde, A. Advances in Solar Energy towards Efficient and Sustainable Energy. *Sustainability* **2021**, *13*, 6295. [CrossRef]
4. Kler, A.M.; Zharkov, P.; Epishkin, N.O. Parametric optimization of supercritical power plants using gradient methods. *Energy* **2019**, *189*, 116230. [CrossRef]
5. Surve, J.; Parmar, J.; Patel, S.K.; Jadeja, R. Comparative analysis of metasurface array-based solar absorber for visible region. *Opt. Quantum Electron.* **2021**, *53*, 696. [CrossRef]
6. Cui, T.J.; Smith, D.R.; Liu, R. *Metamaterials: Theory, Design, and Applications*; Springer: New York, NY, USA, 2010; pp. 1–19, ISBN 9781441905727.
7. Mahmud, S.; Karim, M.; Islam, S.S.; Shuvo, M.K.; Akter, T.; Almutairi, A.F.; Islam, M.T. A Multi-Band Near Perfect Polarization and Angular Insensitive Metamaterial Absorber With a Simple Octagonal Resonator for Visible Wavelength. *IEEE Access* **2021**, *9*, 117746–117760. [CrossRef]
8. Mahmud, S.; Islam, S.S.; Mat, K.; Chowdhury, M.E.H.; Rmili, H.; Islam, M.T. Design and parametric analysis of a wide-angle polarization-insensitive metamaterial absorber with a star shape resonator for optical wavelength applications. *Results Phys.* **2020**, *18*, 103259. [CrossRef]
9. Patel, S.K.; Parmar, J.; Katkar, V. Graphene-based multilayer metasurface solar absorber with parameter optimization and behavior prediction using Long Short-Term Memory model. *Renew. Energy* **2022**, *191*, 47–58. [CrossRef]
10. Huang, H.-L.; Xia, H.; Guo, Z.-B.; Xie, D.; Li, H.-J. Design of Broadband Metamaterial Absorbers for Permittivity Sensitivity and Solar Cell Application. *Chin. Phys. Lett.* **2017**, *34*, 117801. [CrossRef]
11. Abdelraouf, O.A.M.; Shaker, A.; Allam, N.K. Using all dielectric and plasmonic cross grating metasurface for enhancing efficiency of CZTS solar cells. *Nanophotonics VII* **2018**, *10672*, 246–255. [CrossRef]
12. Hoque, A.; Islam, M.T.; Almutairi, A.F.; Faruque, M.R.I. Design of Split Hexagonal Patch Array Shaped Nano-metaabsorber with Ultra-wideband Absorption for Visible and UV Spectrum Application. *Nanoscale Res. Lett.* **2019**, *14*, 1–10. [CrossRef] [PubMed]
13. Patel, S.K.; Parmar, J.; Katrodiya, D.; Nguyen, T.K.; Holdengreber, E.; Dhasarathan, V. Broadband metamaterial-based near-infrared absorber using an array of uniformly placed gold resonators. *J. Opt. Soc. Am. B* **2020**, *37*, 2163. [CrossRef]
14. Parmar, J.; Patel, S.K.; Katrodiya, D.; Nguyen, T.K.; Skibina, J.S.; Dhasarathan, V. Numerical investigation of gold metasurface based broadband near-infrared and near-visible solar absorber. *Phys. B Condens. Matter* **2020**, *591*, 412248. [CrossRef]
15. Nguyen, D.M.; Lee, D.; Rho, J. Control of light absorbance using plasmonic grating based perfect absorber at visible and near-infrared wavelengths. *Sci. Rep.* **2017**, *7*, 2611. [CrossRef]
16. Li, Y.; Li, D.; Zhou, D.; Chi, C.; Yang, S.; Huang, B. Efficient, Scalable, and High-Temperature Selective Solar Absorbers Based on Hybrid-Strategy Plasmonic Metamaterials. *Sol. RRL* **2018**, *2*, 1800057. [CrossRef]
17. Abdulkarim, Y.I.; Alkurt, F.; Awl, H.N.; Altıntaş, O.; Muhammadsharif, F.F.; Appasani, B.; Bakır, M.; Karaaslan, M.; Taouzari, M.; Dong, J. A Symmetrical Terahertz Triple-Band Metamaterial Absorber Using a Four-Capacitance Loaded Complementary Circular Split Ring Resonator and an Ultra-Thin ZnSe Substrate. *Symmetry* **2022**, *14*, 1477. [CrossRef]
18. Dahlberg, O.; Valerio, G.; Quevedo-Teruel, O. Fully Metallic Flat Lens Based on Locally Twist-Symmetric Array of Complementary Split-Ring Resonators. *Symmetry* **2019**, *11*, 581. [CrossRef]
19. Li, X.; Zheng, G.; Zhang, G.; Yang, J.; Hu, M.; Li, J.; Li, Y.; Lu, H.; Yin, Z. Highly Sensitive Terahertz Dielectric Sensor for Liquid Crystal. *Symmetry* **2022**, *14*, 1820. [CrossRef]
20. Naveed, M.A.; Bilal, R.M.H.; Baqir, M.A.; Bashir, M.M.; Ali, M.M.; Rahim, A.A. Ultrawideband fractal metamaterial absorber made of nickel operating in the UV to IR spectrum. *Opt. Express* **2021**, *29*, 42911. [CrossRef]
21. Li, C.; Pan, R.; Geng, G.; Zheng, R.; Gu, C.; Guo, H.; Li, J. Strong and Omnidirectional Light Absorption from Ultraviolet to Near-Infrared Using GST Metasurface. *Laser Photon.-Rev.* **2023**, *17*, 2200364. [CrossRef]
22. Shafique, A.; Naveed, M.A.; Ijaz, S.; Zubair, M.; Mehmood, M.Q.; Massoud, Y. Highly efficient Vanadium Nitride based metasurface absorber/emitter for solar-thermophotovoltaic system. *Mater. Today Commun.* **2023**, *34*, 105416. [CrossRef]

23. Kondaiah, P.; Niranjan, K.; John, S.; Barshilia, H.C. Tantalum carbide based spectrally selective coatings for solar thermal absorber applications. *Sol. Energy Mater. Sol. Cells* **2019**, *198*, 26–34. [CrossRef]
24. Bilal, R.; Baqir, M.; Choudhury, P.; Naveed, M.; Ali, M.; Rahim, A. Ultrathin broadband metasurface-based absorber comprised of tungsten nanowires. *Results Phys.* **2020**, *19*, 103471. [CrossRef]
25. Sun, K.; Riedel, C.A.; Wang, Y.; Urbani, A.; Simeoni, M.; Mengali, S.; Zalkovskij, M.; Bilenberg, B.; de Groot, C.H.; Muskens, O.L. Metasurface Optical Solar Reflectors Using AZO Transparent Conducting Oxides for Radiative Cooling of Spacecraft. *ACS Photon.* **2018**, *5*, 495–501. [CrossRef]
26. Mehrabi, S.; Bilal, R.M.H.; Naveed, M.A.; Ali, M.M. Ultra-broadband nanostructured metamaterial absorber based on stacked square-layers of TiN/TiO_2. *Opt. Mater. Express* **2022**, *12*, 2199. [CrossRef]
27. Lin, K.-T.; Lin, H.; Yang, T.; Jia, B. Structured graphene metamaterial selective absorbers for high efficiency and omnidirectional solar thermal energy conversion. *Nat. Commun.* **2020**, *11*, 1389. [CrossRef]
28. Geim, A.K.; Novoselov, K.S. The rise of graphene. *Nat. Mater.* **2007**, *6*, 183–191. [CrossRef]
29. Patel, S.K.; Charola, S.; Parmar, J.; Ladumor, M.; Ngo, Q.M.; Dhasarathan, V. Broadband and efficient graphene solar absorber using periodical array of C-shaped metasurface. *Opt. Quantum Electron.* **2020**, *52*, 250. [CrossRef]
30. Charola, S.; Patel, S.K.; Parmar, J.; Ladumor, M.; Dhasarathan, V. Broadband graphene-based metasurface solar absorber. *Microw. Opt. Technol. Lett.* **2020**, *62*, 1366–1373. [CrossRef]
31. Olabi, A.; Abdelkareem, M.A.; Wilberforce, T.; Sayed, E.T. Application of graphene in energy storage device—A review. *Renew. Sustain. Energy Rev.* **2021**, *135*, 110026. [CrossRef]
32. Patel, S.K.; Charola, S.; Jani, C.; Ladumor, M.; Parmar, J.; Guo, T. Graphene-based highly efficient and broadband solar absorber. *Opt. Mater.* **2019**, *96*, 109330. [CrossRef]
33. Saurabh, Y.K.; Jha, P.A.; Dubey, P.K.; Jha, P.K.; Singh, P. Bandgap engineering in TiO_2/rGO 1D photonic metasurfaces as broadband solar absorber. *J. Appl. Phys.* **2022**, *131*, 023106. [CrossRef]
34. Parmar, J.; Patel, S.K.; Katkar, V. Graphene-based metasurface solar absorber design with absorption prediction using machine learning. *Sci. Rep.* **2022**, *12*, 2609. [CrossRef] [PubMed]
35. Baqir, M.; Choudhury, P.; Akhtar, M.N. ZrN fractal-graphene-based metamaterial absorber in the visible and near-IR regimes. *Optik* **2021**, *237*, 166769. [CrossRef]
36. Patel, S.K.; Surve, J.; Jadeja, R.; Katkar, V.; Parmar, J.; Ahmed, K. Ultra-Wideband, Polarization-Independent, Wide-Angle Multilayer Swastika-Shaped Metamaterial Solar Energy Absorber with Absorption Prediction using Machine Learning. *Adv. Theory Simul.* **2022**, *5*, 2100604. [CrossRef]
37. Liao, M.; Gao, Y.; Xie, Y.; Zhu, J.; Li, Z.; Tian, W.; Zhu, Z. Investigation on the anti-aging properties enhancement mechanism of graphene on RA based on size effect. *Case Stud. Constr. Mater.* **2022**, *17*, e01634. [CrossRef]
38. Guo, R.; Tang, J.; Gu, J.; Guo, G.; Feng, X. Analysis on the road performance of graphene composite rubber asphalt and its mixture. *Case Stud. Constr. Mater.* **2022**, *17*, e01664. [CrossRef]
39. Ashraf, S.; Khan, S.; Oad, V.K. Microcracking monitoring and damage detection of graphene nanoplatelets-cement composites based on acoustic emission technology. *Case Stud. Constr. Mater.* **2023**, *18*, e01844. [CrossRef]
40. Pereira, P.; Ferreira, D.P.; Araújo, J.C.; Ferreira, A.; Fangueiro, R. The Potential of Graphene Nanoplatelets in the Development of Smart and Multifunctional Ecocomposites. *Polymers* **2020**, *12*, 2189. [CrossRef]
41. Kamedulski, P.; Lukaszewicz, J.; Witczak, L.; Szroeder, P.; Ziolkowski, P. The Importance of Structural Factors for the Electrochemical Performance of Graphene/Carbon Nanotube/Melamine Powders towards the Catalytic Activity of Oxygen Reduction Reaction. *Materials* **2021**, *14*, 2448. [CrossRef] [PubMed]
42. González, Z.; Acevedo, B.; Predeanu, G.; Axinte, S.M.; Drăgoescu, M.-F.; Slăvescu, V.; Fernandez, J.J.; Granda, M.; Gryglewicz, G.; Melendi-Espina, S. Graphene materials from microwave-derived carbon precursors. *Fuel Process. Technol.* **2021**, *217*, 106803. [CrossRef]
43. Selvam, P.P.; Narayanan, R. Random restart local search optimization technique for sustainable energy-generating induction machine. *Comput. Electr. Eng.* **2019**, *73*, 268–278. [CrossRef]
44. Wang, Y.; Wang, P.; Zhang, J.; Cui, Z.; Cai, X.; Zhang, W.; Chen, J. A Novel Bat Algorithm with Multiple Strategies Coupling for Numerical Optimization. *Mathematics* **2019**, *7*, 135. [CrossRef]
45. Li, J.; Lei, H.; Alavi, A.; Wang, G.-G. Elephant Herding Optimization: Variants, Hybrids, and Applications. *Mathematics* **2020**, *8*, 1415. [CrossRef]
46. Eiben, A.; Smit, S. Parameter tuning for configuring and analyzing evolutionary algorithms. *Swarm Evol. Comput.* **2011**, *1*, 19–31. [CrossRef]
47. Song, Y.; Wu, D.; Mohamed, A.W.; Zhou, X.; Zhang, B.; Deng, W. Enhanced Success History Adaptive DE for Parameter Optimization of Photovoltaic Models. *Complexity* **2021**, *2021*, 6660115. [CrossRef]
48. Tyflopoulos, E.; Steinert, M. Topology and Parametric Optimization-Based Design Processes for Lightweight Structures. *Appl. Sci.* **2020**, *10*, 4496. [CrossRef]
49. Patel, S.K.; Parmar, J.; Zakaria, R.B.; Sharafali, A.; Nguyen, T.K.; Dhasarathan, V. Sensitivity Analysis of Metasurface Array-Based Refractive Index Biosensors. *IEEE Sensors J.* **2021**, *21*, 1470–1477. [CrossRef]
50. Patel, S.K.; Parmar, J.; Katkar, V. Metasurface-based solar absorber with absorption prediction using machine learning. *Opt. Mater.* **2022**, *124*, 112049. [CrossRef]

51. Alsaif, H.; Patel, S.K.; Ben Ali, N.; Armghan, A.; Aliqab, K. Numerical Simulation and Structure Optimization of Multilayer Metamaterial Plus-Shaped Solar Absorber Design Based on Graphene and SiO_2 Substrate for Renewable Energy Generation. *Mathematics* **2023**, *11*, 282. [CrossRef]
52. Yu, P.; Chen, X.; Yi, Z.; Tang, Y.; Yang, H.; Zhou, Z.; Duan, T.; Cheng, S.; Zhang, J.; Yi, Y. A numerical research of wideband solar absorber based on refractory metal from visible to near infrared. *Opt. Mater.* **2019**, *97*, 109400. [CrossRef]
53. Lin, H.; Sturmberg, B.C.P.; Lin, K.-T.; Yang, Y.; Zheng, X.; Chong, T.K.; de Sterke, C.M.; Jia, B. A 90-nm-thick graphene metamaterial for strong and extremely broadband absorption of unpolarized light. *Nat. Photon.* **2019**, *13*, 270–276. [CrossRef]
54. Azad, A.K.; Kort-Kamp, W.J.M.; Sykora, M.; Weisse-Bernstein, N.R.; Luk, T.S.; Taylor, A.J.; Dalvit, D.A.R.; Chen, H.-T. Metasurface Broadband Solar Absorber. *Sci. Rep.* **2016**, *6*, 20347. [CrossRef]
55. Liu, B.; Tang, C.; Chen, J.; Xie, N.; Tang, H.; Zhu, X.; Park, G.-S. Multiband and Broadband Absorption Enhancement of Monolayer Graphene at Optical Frequencies from Multiple Magnetic Dipole Resonances in Metamaterials. *Nanoscale Res. Lett.* **2018**, *13*, 153. [CrossRef]
56. Sang, T.; Gao, J.; Yin, X.; Qi, H.; Wang, L.; Jiao, H. Angle-Insensitive Broadband Absorption Enhancement of Graphene Using a Multi-Grooved Metasurface. *Nanoscale Res. Lett.* **2019**, *14*, 105. [CrossRef]
57. Rufangura, P.; Sabah, C. Graphene-based wideband metamaterial absorber for solar cells application. *J. Nano Photon.* **2017**, *11*, 036008. [CrossRef]
58. Liu, Y.; Chen, Y.; Li, J.; Hung, T.-C.; Li, J. Study of energy absorption on solar cell using metamaterials. *Sol. Energy* **2012**, *86*, 1586–1599. [CrossRef]
59. Patel, S.K.; Charola, S.; Parmar, J.; Ladumor, M. Broadband metasurface solar absorber in the visible and near-infrared region. *Mater. Res. Express* **2019**, *6*, 086213. [CrossRef]